

# An experimental study of unstable barotropic vortices in a rotating fluid

By R. C. KLOOSTERZIEL† AND G. J. F. VAN HEIJST

Institute of Meteorology and Oceanography, University of Utrecht, Princetonplein 5,  
3584 CC Utrecht, The Netherlands

(Received 13 April 1990)

Laboratory experiments on barotropic vortices in a rotating fluid revealed that the instability behaviour of cyclonic and anticyclonic vortices is remarkably different. Depending on its initial vorticity distribution, the cyclonic vortex has in a number of experiments been observed to be unstable to wavenumber-2 perturbations, leading to the gradual formation of a stable tripolar vortex structure. This tripole consists of an elongated cyclonic core vortex adjoined by two anticyclonic satellite vortices.

In contrast, the anticyclonic vortex shows a rather explosive instability behaviour, in the sense that it is observed to immediately split up into two dipoles. Under somewhat different circumstances the higher-order mode-3 instability is observed, in which the anticyclonic core has a triangular shape, with three smaller cyclonic satellite vortices at its sides.

A modified version of Rayleigh's instability criterion offers a qualitative explanation for this apparent difference between unstable cyclonic and anticyclonic vortices.

---

## 1. Introduction

The occurrence of large-scale eddies is a well-known feature of the world's oceans, and observations by satellites have provided essential information about their formation, their lifetime, and their spatial distribution. Ocean eddies, or vortices, are generated in various ways, for instance by separation from meandering currents (e.g. the Gulf Stream or the Algalhas Current) or by separation from unstable coastal currents (e.g. the Norwegian Coastal Current). An extensive collection of examples of oceanic eddies can be found in Robinson (1983). It is obvious from their large dimensions (10 to 100 km, typically) and their relatively long lifetime – in some cases a couple of years – that vortices play an important role in the transport of properties such as heat, salt and biochemical components. For this reason considerable effort is being put in studying the dynamics of large-scale vortices. Although the approach to the problem is mainly theoretical, i.e. by performing numerical simulations and by applying analytical techniques, the dynamics of vortices in a rotating fluid system has also been investigated experimentally. An important question concerns the stability of vortices, and this aspect has been studied in the laboratory by Saunders (1973) and Griffiths & Linden (1981) for the case of baroclinic two-layer vortices. For some reason the behaviour of isolated *barotropic* vortices in a rotating fluid has received much less attention, as far as we

† Present affiliation: Institute for Nonlinear Science, La Jolla, CA 92093, USA.

are aware. The present authors have carried out experiments on barotropic vortices in a rotating fluid, and this work has revealed a number of interesting properties not observed in the baroclinic cases. Part of the work was concentrated on the behaviour of stable barotropic vortices, i.e. vortices that remained circularly symmetric throughout their decay. It was found that a combination of two effects plays a crucial role in the dynamics of the decay process, viz. the action of the bottom Ekman layer and the deformability of the free upper surface. Results of this experimental and theoretical work will be published separately (Kloosterziel & van Heijst 1990).

Along with the study of stable barotropic vortices, experiments were performed in which the behaviour of their unstable counterparts was examined. Under certain conditions the unstable cyclonic vortex showed a gradual transition to a stable tripolar vortex structure, a phenomenon already described by van Heijst & Kloosterziel (1989) and in more detail by Kloosterziel & van Heijst (1989) and by van Heijst, Kloosterziel & Williams (1991). In dramatic contrast to this tripole formation, the unstable anticyclonic vortex is generally observed to split up, often into two dipoles that move away from the original vortex centre. Although the details of this remarkable difference in stability behaviour are not yet well understood, it was found that an extended version of Rayleigh's instability criterion (for vortex flow in a rotating fluid) agrees, in a qualitative sense, with the laboratory observations.

In a number of experiments it was observed that the anticyclonic vortex was unstable to a wavenumber-3 perturbation, giving rise to a vortex structure consisting of a triangular anticyclonic core with three smaller cyclonic satellite vortices beside it. This structure appeared to be unstable, however, and broke up into two vortex dipoles.

Preceded by a description of the experimental set-up (§2), these observations are described in §3 of this paper. The instability is considered in §4, and criteria for instability of cyclonic and anticyclonic vortices are derived from a modified version of Rayleigh's (circulation) theorem.

## 2. Laboratory arrangement

In order to study the dynamics of barotropic vortices in a rotating fluid, laboratory experiments have been conducted in which vortices were generated by using a few essentially different techniques. A convenient way of creating vortices is by applying the so-called 'collapse technique', the basic set-up for which is shown in figure 1: the rotating tank is filled with a homogeneous fluid, and a bottomless cylinder is placed concentrically in the tank, with the fluid inside the inner cylinder at a level differing from that outside it. When the inner cylinder is withdrawn vertically, a gravity-driven flow will arise in radial direction. This radial motion is deflected by the Coriolis force, such that after a period of typically  $\pi/\Omega$  ( $\Omega$  being the angular velocity of the turntable) an equilibrium state is reached in which the flow is purely azimuthal. In this state the azimuthal flow is governed by a balance between radial forces, viz. the centrifugal force, the Coriolis force, and the radial pressure-gradient force. This balance is usually referred to as 'gradient flow' (see Holton 1979). In particular when the difference in level  $\Delta H$  is of the same order of magnitude as the average water depth, lifting of the cylinder usually results in a vigorous turbulent flow in the centre of the tank. Although this flow is initially three-dimensional, visibly involving vertical motions, after typically 2–3 rotation periods the fluid motion is observed to become nearly two-dimensional, taking the

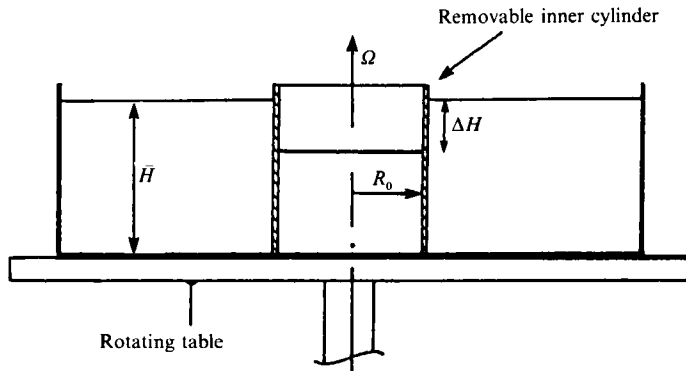


FIGURE 1. A schematic drawing of the laboratory set-up used for producing barotropic vortices.

appearance of a horizontal swirl flow around the axis. As can be understood from conservation of angular momentum, cyclonic vortices are created when the fluid level inside the inner cylinder is lower than outside, whereas a higher central fluid level in principle should result in an anticyclonic flow.

In a number of additional experiments cyclonic vortices were created in an alternative way, by locally stirring the fluid with a thin rod. This could be done most conveniently by briefly stirring the fluid confined in the central bottomless cylinder, which – after allowing the stirring-induced motion to become organized in a purely azimuthal vortex flow – was lifted vertically. In this way both cyclonic and anticyclonic vortices were produced.

The experiments described in the present paper were performed in a cylindrical Perspex tank, 92.5 cm in diameter and 30 cm deep, placed on top of a 1 m diameter rotating table (see figure 1). The working depth  $\bar{H}$  of the tank (measured at rest) was varied between 5 cm and 25 cm. Two different inner cylinders were used, with 29.0 cm and 11.0 cm internal diameters  $2R_0$ , and the Coriolis parameter  $f \equiv 2\Omega$  (in  $\text{rad s}^{-1}$ ) was varied in the range  $0.87 \text{ s}^{-1}$  to  $1.98 \text{ s}^{-1}$ . The flows were visualized by addition of tracer particles floating on the fluid surface, and by adding dye. Velocity measurements were performed by means of streak photography of the tracer particles; for this purpose a remotely controlled photo camera was mounted in the rotating frame at some distance above the fluid surface. Velocities were calculated by measuring the lengths of the streaks on the photographs. Qualitative information about the flow below the surface was obtained by dropping dye-producing crystals in the tank and observing the subsequent distortion of their dye trails.

### 3. Observations of unstable vortices

Before describing the instability behaviour of vortices as observed in the laboratory experiments, it is necessary to make some remarks about the general structure of the initially circularly symmetric, monopolar vortices (we use the term monopolar here to mean that the vortex consists of a single set of nested closed streamlines and not, as some authors do, that the vorticity is one-signed). The velocity field of the initial vortex and its subsequent evolution can be reconstructed quantitatively from the streak photographs by measuring the lengths of the streaks, and dividing these by the exposure time. For a typical axisymmetric cyclonic vortex the measured azimuthal velocity  $v$  is plotted in figure 2(a) as a function of the radius

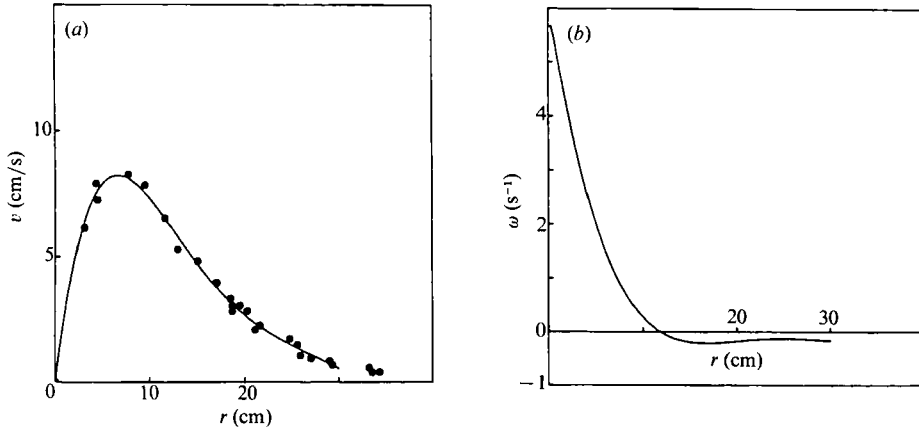


FIGURE 2. (a) The radial distribution of the azimuthal velocity of a typical cyclonic, barotropic vortex. Measured velocities are indicated with black dots while the solid line is a fourth-order polynomial. (b) The corresponding radial vorticity distribution, derived from the polynomial approximation of the velocity field.

$r$ , as measured from the vortex centre. The experimental data are shown by dots, and the solid line is a fourth-order polynomial that has been fitted by means of a least-squares approximation. The radial distribution of the relative vorticity

$$\omega(r) = \frac{1}{r} \frac{d}{dr}(rv)$$

is then easily calculated by using the polynomial fit as a representation of  $v(r)$ . Figure 2(b) shows the vorticity profile associated with the experimental data of figure 2(a). Obviously, the vortex has a core of positive relative vorticity, which is surrounded by a ring of negative relative vorticity. It was found in the experiments that this vorticity distribution depends to some degree on the generation technique applied. For example, in some cases the outer ring of negative vorticity turned out to be rather narrow, with the negative vorticity having a relatively large magnitude. In other cases this ring appeared to be much wider, and the negative vorticity magnitude correspondingly weaker. Similar remarks apply to anticyclonic vortices, but with ‘cyclonic’ everywhere replaced by ‘anticyclonic’, ‘negative’ by ‘positive’, and so on. The laboratory vortices studied in this paper were generally isolated, i.e. had vanishing circulation for large enough radii. In accordance with results obtained by Flierl (1988) in an analytical study of the linear stability properties of similar but strongly simplified vortices (with piecewise-constant vorticity in the core and the ring), the observed instability behaviour depends very much on the shape of the vorticity distribution in the initial stage, i.e. before the vortex loses its axisymmetry. This was also shown numerically by Gent & McWilliams (1986) for isolated vortices with continuously distributed vorticity. In both studies the flow was assumed to be purely two-dimensional; the stability properties of vortices do not depend on the sign of the vortex in such flows, i.e. on whether they are cyclones or anticyclones. The fact that the stability behaviour of cyclones and anticyclones in the laboratory is quite different, as is described below, thus implies that three-dimensional effects in the rotating tank cannot be excluded from stability considerations.

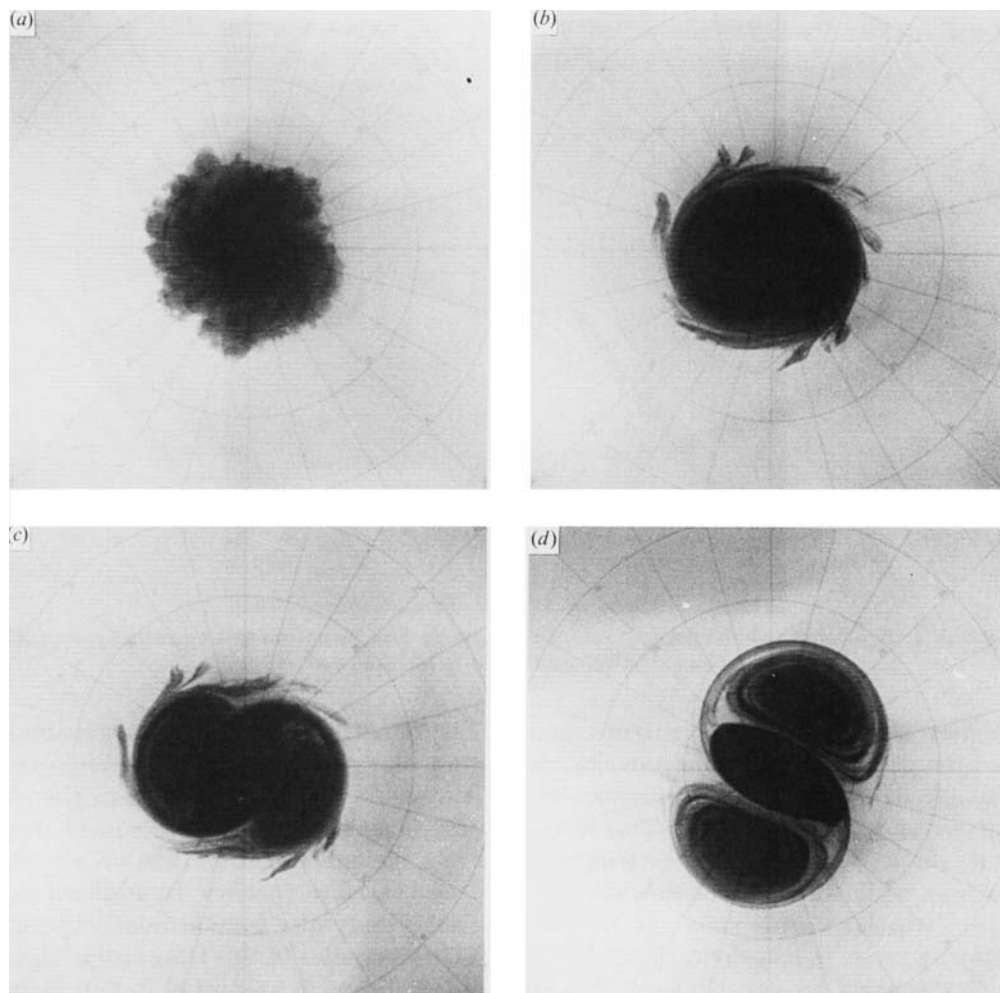


FIGURE 3. The evolution of an unstable cyclonic stirring-induced barotropic vortex into a stable tripolar structure. The photographs were taken at (a)  $t = 0.6T$ , (b)  $7.2T$ , (c)  $9.0T$  and (d)  $17.3T$  after releasing the vortex, with the rotation period of the turntable  $T = 8.4$  s. The initial vortex diameter was 11 cm and the mean water depth measured 15 cm.

### 3.1. *Stirring-induced vortices*

Both cyclonic and anticyclonic vortices were generated by the stirring technique as described in §2. It was found in all cases that the vortices thus produced were unstable and showed a rapid transition to non-axisymmetric patterns: the cyclonic stirring vortices were seen to transform into a tripolar flow structure, whereas the anticyclonic vortices generally broke up into a set of two dipole structures.

The typical evolution of a *cyclonic* barotropic stirring vortex is illustrated by the photographs shown in figure 3. For the purpose of flow visualization in this experiment, dye was added to the stirred fluid in the inner cylinder. Immediately after releasing the vortex by lifting the inner cylinder, vigorous turbulent mixing occurred at the circumference of the vortex. This can easily be observed in figure 3(a), where the dyed patch has a rather irregular appearance. After a few rotation periods, however, the flow settled to an approximately circular vortex, see figure 3(b). Careful observation of the dye concentration in this photograph reveals a

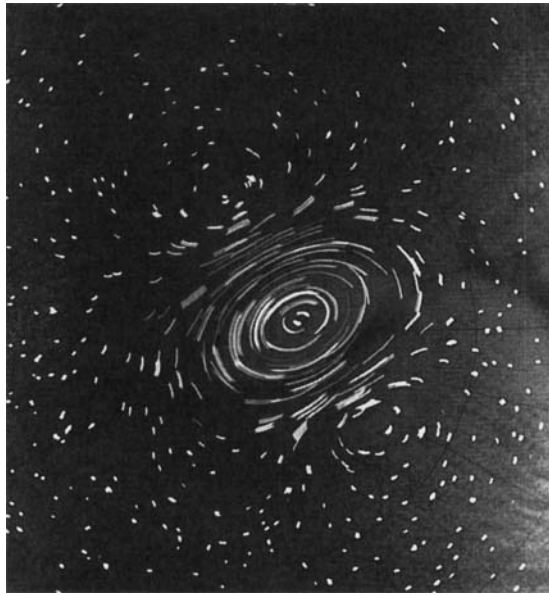


FIGURE 4. Typical streakline photograph of the tripolar flow structure arising from an unstable cyclonic, stirring-induced barotropic vortex.

slightly asymmetric flow structure, and this asymmetry becomes more pronounced as time progresses. As illustrated by figure 3(c), the vortex shows a transition to a tripolar structure, and the eventual tripole can clearly be distinguished in the dye pattern shown in figure 3(d). This flow structure is persistent, and shows no changes in its shape. The motion in the tripole core is in a cyclonic direction (like the original vortex), while anticyclonic flow occurs in the two satellite vortices. In addition, the entire tripolar vortex structure rotates in a solid-body-like fashion relative to the rotating frame in a cyclonic direction. Some characteristics of this laboratory tripole were discussed by van Heijst & Kloosterziel (1989) and Kloosterziel & van Heijst (1989). For experiments like the one shown in figure 3, the Rossby number of the initial vortex typically lies in the range 1–3.

In a numerical study of perturbed ‘minimum-*enstrophy* vortices’, Leith (1984) found evidence for the emergence of a tripole structure, and in a brief remark he mentioned that the strengths of the vortices in the tripole measured roughly  $(-1, 2, -1)$ . If – in a simplifying approach – the tripole were modelled by a combination of three aligned point vortices with these strengths, one would indeed find a cyclonic rotation of this vortex constellation, in accordance with the laboratory observations. The flow pattern associated with such a tripolar vortex set has been calculated, and plotted results are presented by Kloosterziel & van Heijst (1989).

Recently, an example of a tripole was found by Legras, Santangelo & Benzi (1988) in numerical experiments on forced two-dimensional turbulence, and their numerically obtained tripole structure shows much resemblance to the dye pattern visible in figure 3(d). Other numerical studies that showed the emergence of tripoles under certain circumstances have been reported by, for example, Ikeda (1981), Swenson (1987) and Carton, Flierl & Polvani (1989). However, no observational evidence of the occurrence of tripoles in nature seems to have been reported before.

The tripolar flow arising from an unstable stirring-induced cyclonic vortex was also visualized by streakline photographs of small tracer particles floating on the free

surface of the fluid, and an example of the observed particle paths is presented in figure 4. It is obvious that the streaklines indicate a tripolar pattern, but experiments with both dye and tracer particles revealed that the dye pattern does not coincide with the streakline pattern: although the axes of both tripolar patterns coincided, in particular the satellite vortices in the dye pattern were observed to occupy a considerably smaller area than those visible in the streakline picture. The reason for this discrepancy lies in the solid-body rotation of the tripole, which obviously induces (irrotational) relative motion at some distance from the dyed region. If the streakline photographs were to be analysed in order to determine the flow field associated with the tripole, a correction should be made for its rotation. In fact, appropriate data reduction techniques are being developed and some preliminary results are presented by Kloosterziel & van Heijst (1989). Further details of tripolar laboratory vortices will be published elsewhere (van Heijst *et al.* 1991).

The behaviour of an *anticyclonic* stirring-induced barotropic vortex is entirely different from its cyclonic counterpart, and the sequence of events as observed in the laboratory experiments is shown in figure 5. The first photograph (*a*) is taken just after lifting the inner cylinder in which the stirred (dyed) fluid was confined, and – as in the previous experiment – the irregular appearance of the dye blob indicates turbulent mixing with the ambient fluid. Its slightly elongated appearance indicates that a wavenumber-2 perturbation has already grown to a finite amplitude, and soon thereafter two *cyclonic* vortices are seen to emerge from the dyed region, see figure 5(*b, c*), and these move in opposite directions away from the centre. Comparison of the photographs shown in (*b*) and (*c*) reveals that the motion of the vortices is not purely radial: the vortices show an additional drift in an anticyclonic direction. In the next stage, see (*d*), anticyclonic vorticity is seen to become concentrated into a small eddy on one side of each cyclonic vortex, leading to the formation of two dipole structures, as can be observed on (*e*). These dipole structures are somewhat asymmetric, the cyclonic parts being stronger than the anticyclonic parts. For this reason and owing to the presence of the tank wall, the dipoles do not move radially outwards, but they make a looping excursion in a cyclonic direction, back to the tank centre, as can be seen on (*f*). The Rossby number for experiments as shown in figure 5 was typically  $O(1)$ . In a numerical study of unstable barotropic vortices, Flierl (1985, 1988) found a similar behaviour with a vortex breaking up into two dipolar structures, and his vorticity maps calculated for the successive stages of the break-up process show a remarkable resemblance to the dye concentrations observed in the laboratory experiments shown in figure 5. Other numerical studies showing dipole splitting are discussed by, for example, Ikeda (1981), Swenson (1987), Gent & McWilliams (1986), Stern (1987) and Polvani & Carton (1990). Evidence of dipole splitting in ‘nature’ (i.e. in the laboratory) has previously been described by Ginsburg *et al.* (1987) but not in much detail.

In a number of additional experiments stirring vortices were created in a two-layer fluid, and even in the case of a thin bottom layer of slightly larger density, their behaviour appeared to be essentially different from their barotropic counterparts. In cyclonic baroclinic vortices, the raised interface takes on a dome-like shape, and the bottom layer apparently stabilizes the vortex: it remains axisymmetric with circular streamlines, and *no* transition to non-axisymmetric patterns has been observed. On the other hand, the anticyclonic, stirring-induced vortices were observed to be highly unstable, again, as in the barotropic case discussed above. Since the bottom layer effectively shields the upper layer from the strong bottom Ekman layer (the interfacial Ekman layer is much weaker), these results may indicate that the

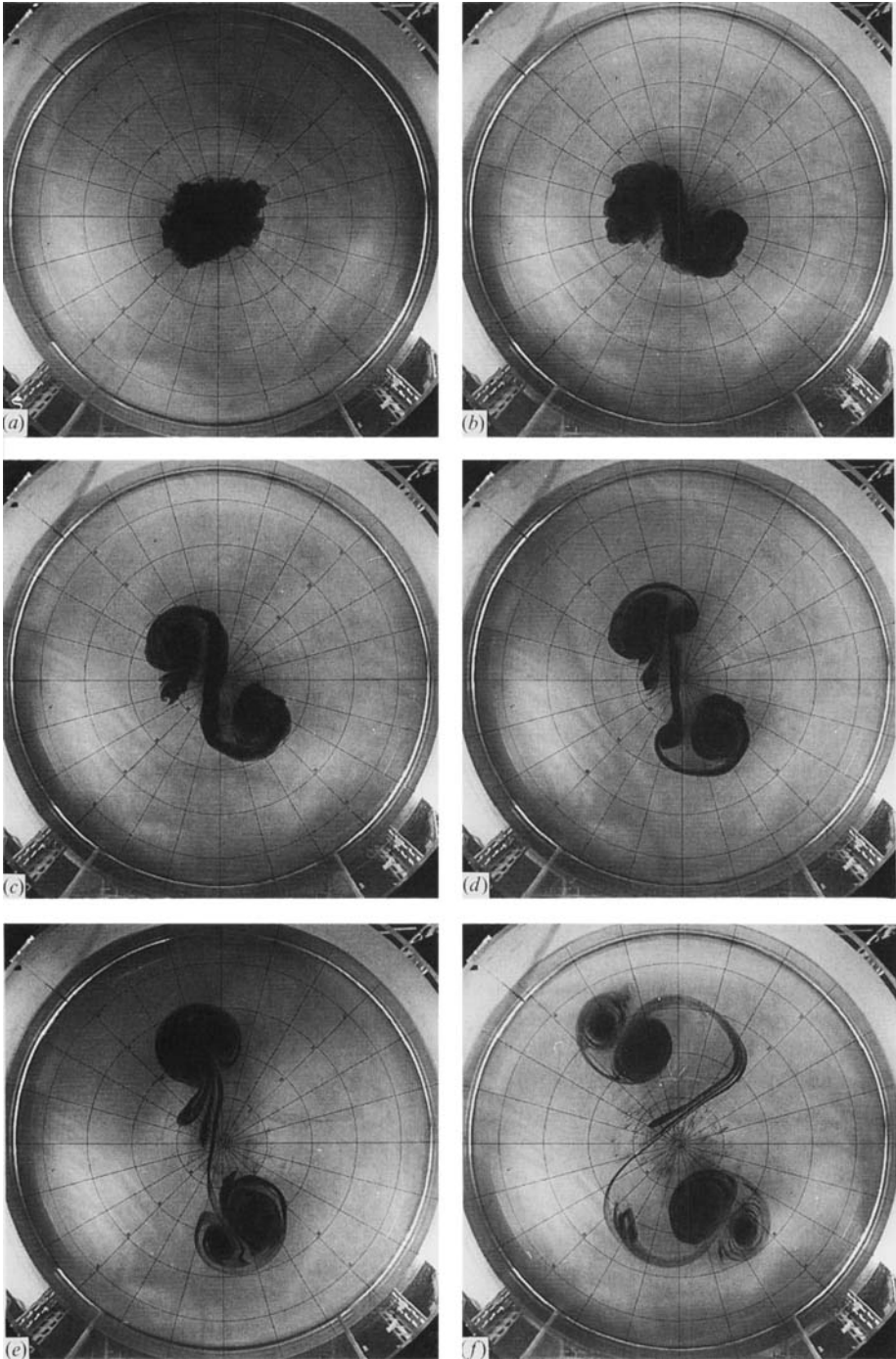


FIGURE 5. The evolution of an unstable anticyclonic, stirring-induced barotropic vortex. The photographs were taken at (a)  $t = 0.6T$ , (b)  $1.9T$ , (c)  $2.9T$ , (d)  $4.1T$ , (e)  $6.2T$  and (f)  $16.7T$  after releasing the vortex, with  $T = 6.3$  s. The initial vortex diameter was 11 cm and the mean water depth 13.3 cm.

instability of the barotropic cyclonic vortices is related to the advective action of the interior Ekman circulation, which is known to change the velocity and vorticity distribution of a vortex considerably, and which thus can bring a vortex into a critical form that is unstable to two-dimensional disturbances, as will be discussed in §4.

The immediate instability of anticyclonic stirring vortices in both the barotropic and baroclinic cases indicates that centrifugal instability could be a trigger for this instability behaviour. The fact that the subsequent events show so much resemblance to what is observed in the above-mentioned two-dimensional simulations does not in itself prove that the underlying causes for the observed behaviour are the same. In fact, dipole splitting has also been noted to occur in the case of unstable two-layer baroclinic vortices in the laboratory (see Griffiths & Linden 1981) and in numerical experiments on baroclinic vortices (see Carton & McWilliams 1989). In §4 it will be shown that Rayleigh's circulation theorem, extended to a rotating system or an  $f$ -plane, can partially explain the different stability behaviour of cyclonic and anticyclonic vortices.

In a number of stirring experiments anticyclonic vortices were produced with small Rossby numbers. Since by simply stirring the liquid in the inner cylinder one usually creates a vortex that has a Rossby number that is not truly small, the flow in the inner cylinder was left to decay for a while before withdrawing the cylinder. In most cases an immediate instability set in, usually with a dominant  $m = 2$  component, which led to dipole splitting, but in a few cases a wavenumber-3 perturbation grew to a finite amplitude instead. This is clearly recognized in the streakline photographs presented in figure 6. The first photograph was taken only 5 s after the vortex was released and already a distinctive deformation of circular symmetry is observed. A dominant wavenumber is not easily recognized in figure 6(a), but in figure 6(b) an  $m = 3$  component is clearly visible as well as in the next two frames. The time exposure of these photographs was 1 s, and an estimate of the Rossby number  $\epsilon$  based on the streakline lengths gives  $\epsilon \sim 0.6$ – $0.7$ . By comparing the subsequent photographs it is seen that this  $m = 3$  vortex is *not* stationary in the tank, and the structure rotates in anticyclonic direction. The motion in the core of the vortex is anticyclonic (clockwise) whereas the three satellites are cyclonic vortices. An interesting and important feature of this vortex is that the amplitude of peak vorticity of the core vortex is of the same order of magnitude as that of the satellite vortices. Measurements showing this are discussed elsewhere (see Kloosterziel 1990), but here it may be noted that in tripoles as discussed in §3.1 the amplitudes of the vorticity of the core and the satellites differ by at least a factor 5 shortly after they have formed. This indicates that the initial conditions leading to tripole formation and triangular vortex formation differ at least in that the ratio of the amplitude of peak vorticity (positive and negative) is much larger in one case than in the other case. In §4 some studies are cited that have shown that isolated vortices with narrow rings of high-amplitude vorticity surrounding the core are more unstable to higher-wavenumber perturbations than vortices with a broader ring of low-amplitude vorticity. Since the anticyclones that transformed into triangular vortices were usually confined to the inner cylinder for a prolonged period of time in order to have a small Rossby number, it seems likely that the Ekman circulation is responsible for setting up a special initial condition not attainable by direct stirring.

At present no detailed analysis has yet been carried out concerning the evolution of vorticity of anticyclones and nothing really precise is known about the initial flows that show triangular-vortex formation in the laboratory. Which wavenumber is the

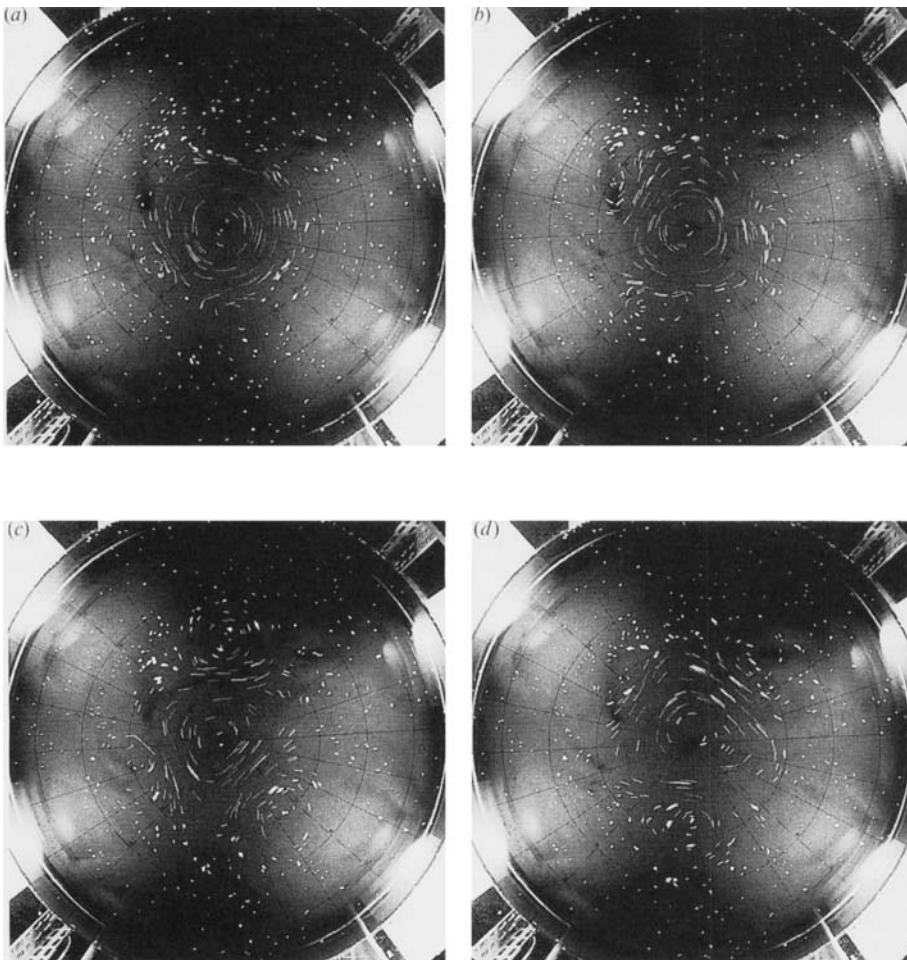


FIGURE 6. Streakline photographs showing the evolution of a low-amplitude anticyclonic stirring vortex. Pictures were taken at (a)  $t = 0.4T$ , (b)  $0.9T$ , (c)  $1.4T$  and (d)  $2.2T$  after releasing the vortex, with  $T = 11.6$  s. The vortex was created by stirring in a cylinder with a diameter of  $2R_0 = 29$  cm. The mean water depth was  $\bar{H} = 15$  cm,  $\Omega = 0.54$  s $^{-1}$  and the exposure time 1 s.

fastest growing one seems to be sensitively dependent on the precise initial conditions. In the laboratory this is reflected by the fact that whenever the experiment is repeated a few times (since the stirring is done by hand, the precise initial conditions are never the same) only now and then does an  $m = 3$  perturbation amplify. It is for this reason that few examples have been found of this particular vortex type.

In figure 7 the sequence of events that followed what is seen in figure 6 is shown. In figure 7(a) the triangular vortex is still as it was before, but soon thereafter two of the cyclonic satellites merged, leading to the formation of an anticyclonic tripole (see figure 7b). This tripole in turn became unstable, as is seen in figure 7(c), and this led to a splitting of the vortex into two dipoles (figure 7d). The same sequence of events has also been observed for much smaller vortices, and this big vortex was only chosen because it provided the clearest streakline photographs; the instability is not forced upon the vortex by boundary effects. The triangular vortex seems not to have been reported before, and the reason for this could be that it is always unstable. This

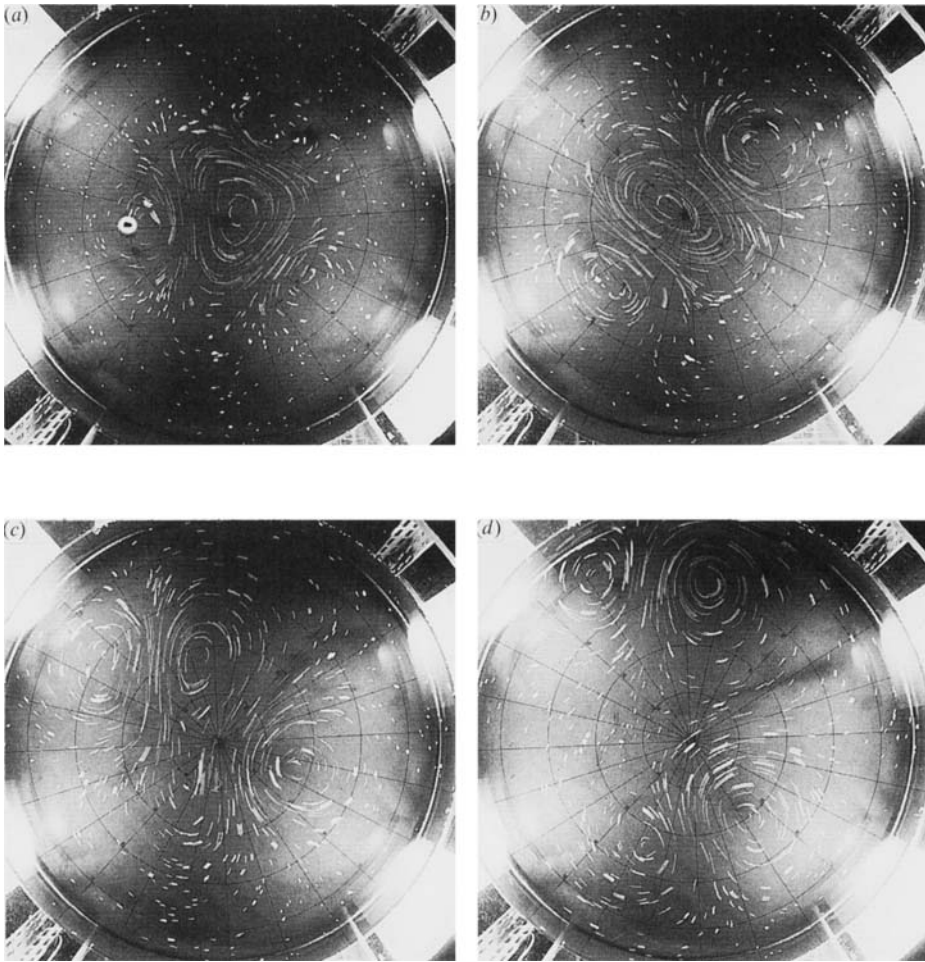


FIGURE 7. A sequence of streakline photographs showing the further evolution of the triangular vortex shown in figure 6(*d*). The photographs were taken at (*a*)  $t = 3.4T$ , (*b*)  $6.0T$ , (*c*)  $7.8T$  and (*d*)  $10.3T$ . Further details are given in the caption of figure 6. Exposure times were: (*a*) 2 s, (*b*, *c*) 3 s, and (*d*) 4 s.

is not clear as yet and maybe stable triangular vortices do exist, but in view of the frequency at which tripoles and dipoles are observed, it is expected to be a much rarer coherent vortex type.

### 3.2. *Off-centre, stirring-induced vortices*

Barotropic stirring-induced vortices were also created at some distance from the rotation axis, and these experiments revealed a number of interesting features. After releasing a cyclonic stirring vortex by lifting the cylinder, vigorous turbulent mixing occurred as in the experiment with a centred vortex (see figure 3), soon resulting in a regular, almost axisymmetric vortex flow. This can be clearly seen on the photographs presented in figure 8(*a*, *b*). Within a few rotation periods, however, the cyclonic vortex starts to propagate towards the centre of the container. On its way to the centre, the vortex shows a transition to a slightly asymmetric tripole structure, leaving behind a weak anticyclonic vortex that slowly moves in an

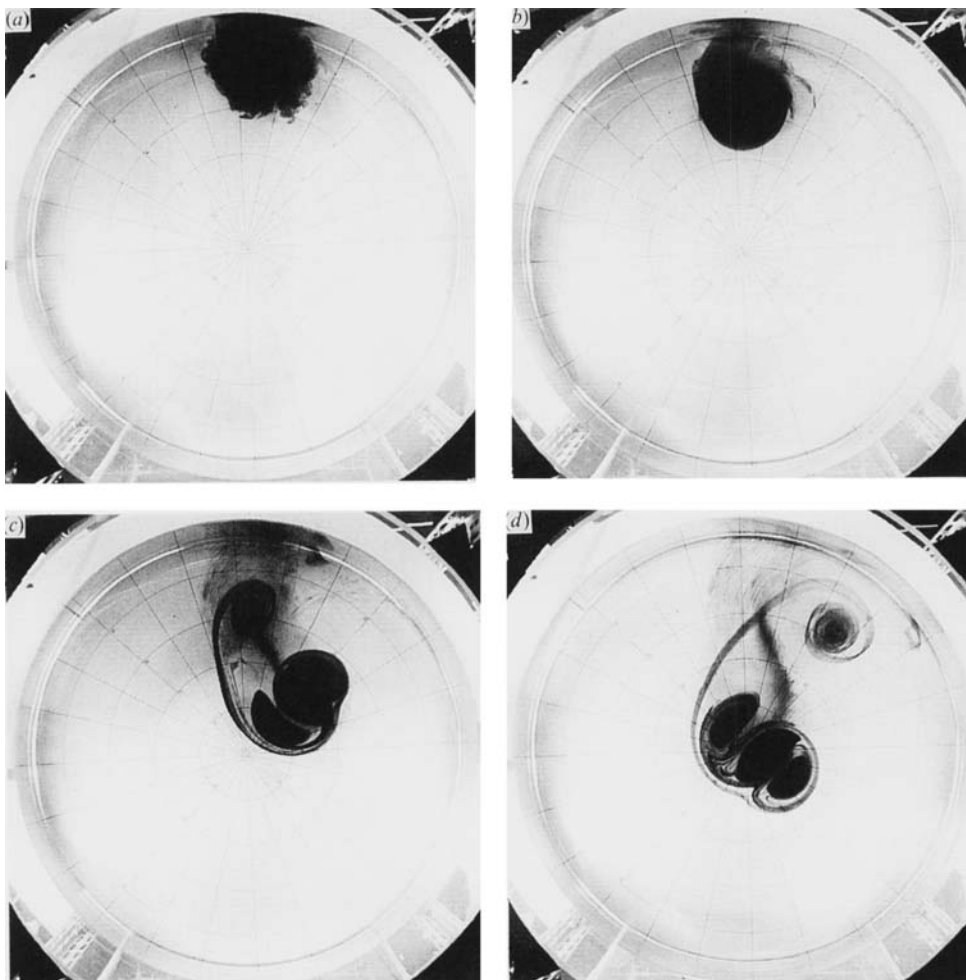


FIGURE 8. The evolution of a cyclonic, stirring-induced barotropic vortex released at a position some distance away from the tank centre. The photographs were taken at (a)  $t = 0.5T$ , (b)  $4.5T$ , (c)  $11.6T$  and (d)  $21.3T$  after the vortex was released, with  $T = 6.28$  s. The initial vortex diameter was 11 cm and the mean water depth 15 cm.

anticyclonic direction (see figure 8c). In the final stage, as illustrated by the photograph in figure 8(d), the tripole has reached the tank centre and rapidly becomes symmetric, like the tripole shown in figure 3.

Careful observation of the dye patterns in consecutive photographs reveals the existence of a weak overall anticyclonic flow in the rotating tank: this is easily observed from the anticyclonic drift of the anticyclonic vortex left at the rim of the tank (boundary effects are possibly involved here), but also from the apparent anticyclonic rotation of the (cyclonic) tripole structure at the centre. The anticyclonic flow is likely to be caused by the translation of the cyclonic vortex towards the centre: ambient fluid is forced to flow away from the centre, resulting – as can be understood from conservation of angular momentum – in anticyclonic motion. The anticyclonic flow can also be observed from the dye streaks originating from some dye-producing crystals left at the bottom at the initial position of the stirring vortex: the dye in the bottom Ekman layer spirals radially outwards in an anticyclonic

direction, which indirectly indicates anticyclonic flow in the fluid column above the bottom layer. Also, the dye on the tank bottom nicely visualizes the track followed by the tripole on its way to the centre. Obviously, this track is not purely in radial direction, and seems to be slightly affected by the overall anticyclonic flow.

The crucial features in this experiment, being the translation towards the rotation axis and the formation of a tripolar vortex structure, appear to be reproducible very well, and have in fact been observed in a number of experimental runs with stirring-induced vortices of varying intensities. It was found, however, that the translation of the vortex and the tripole formation are characterized by timescales that are not necessarily equal. For example, in a few runs the cyclonic vortex was seen to translate towards the rotation axis without losing axisymmetry, and a transition to a tripolar shape was not observed until the vortex had reached the centre of the container. In particular the most energetic vortices showed this behaviour, whereas the weaker vortices became tripoles before reaching the rotation axis (as in figure 8).

The observed inward motion is analogous to the propagation of vortices over topography as is discussed by Carnevale *et al.* (1988). In this numerical study it was observed that cyclones tend to ascend topographic hills in an anticyclonic spiral. It has been plausibly suggested that this phenomenon is in fact equivalent to the northwest motion of cyclonic monopoles on a northern-hemisphere  $\beta$ -plane (see McWilliams & Gent 1986). In both cases, conservation of potential vorticity leads to a dipolar perturbation field on the initially monopolar vorticity structure, which in turn leads to an overall motion towards the northwest (for flows over topography, the compass directions are defined by the local gradient of the topography). Effectively, the parabolic shape of the free surface in our experiments acts as a parabolic topographic feature. Further experiments with cyclonic sink vortices, which were stable and did not transform into tripoles, revealed nice anticyclonic spiralling motions towards the tank centre (see Carnevale, Kloosterziel & van Heijst 1990, for some other examples of topographically induced motion of barotropic vortices). The fact that the stirring vortices while translating simultaneously transform into tripoles, indicates that the overall motion is typically an integral property that is rather insensitive to the precise details of the structure of the vortex.

The vortex motion towards the tank centre as observed for the barotropic cyclonic vortices is in a way similar to the observed uphill motion of baroclinic vortices on a sloping bottom in the laboratory experiments by Mory, Stern & Griffiths (1987): in both cases the vortex shows a tendency to minimize its height. The uphill displacement of the vortex was attributed by these authors both to frictional effects associated with the Ekman layer at the bottom, and to the asymmetry in vortex stretching in the up-slope direction. By using a cover, and therewith flattening the free surface, it was found in our experiments, however, that the barotropic vortices no longer move towards the tank centre. Since, effectively, the influence of the Ekman dynamics doubles in this case, it follows that the Ekman layer(s) should play a negligible role in an explanation for the observed translation of the barotropic vortices.

### 3.3. Vortices produced by gravitational collapse

Under certain conditions the barotropic vortices produced by the collapse technique as described in §2 became unstable too, in the sense that they lost axisymmetry. Unstable cyclonic vortices – generated by the fluid level inside the inner cylinder being lower than outside – were generally seen to show a gradual transition from a circularly symmetric flow pattern to an elliptical structure. In some cases the streamline pattern appeared to change back and forth between circular and elliptical

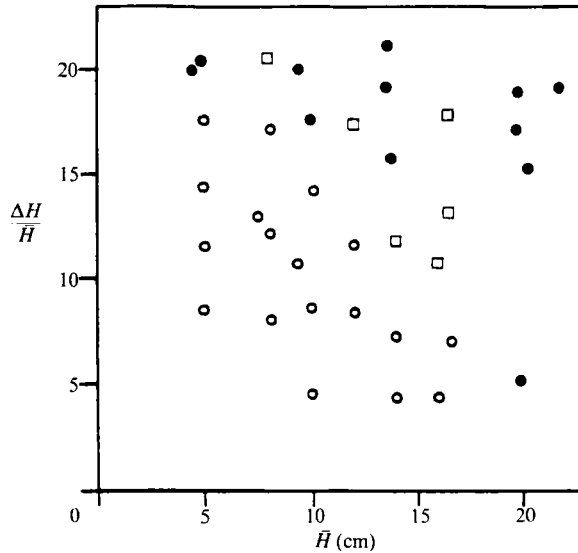


FIGURE 9. The ultimate vortex structure, observed in experiments on cyclonic barotropic vortices created with the collapse technique, as a function of the mean water depth  $\bar{H}$  and the relative initial level difference  $\Delta H/\bar{H}$ . The symbol  $\bullet$  refers to circular and elliptical vortices, whereas  $\circ$  refers to clearly discernible tripolar vortices. Very weak tripoles, that is, vortices with very narrow regions of anticyclonic motion, are indicated  $\square$ . For a further discussion of this diagram, see text.

shapes, a behaviour similar to that found in a study by Cushman-Roisin, Heil & Nof (1985). In other cases, the pinching of the ellipse continued, eventually leading to a stable *tripolar* streamline pattern identical to the ones observed in the experiments with stirring-induced vortices (cf. figure 3). The experiments revealed that, once a tripole structure was formed, this flow pattern was persistent, indicating the stability of these tripoles.

In order to investigate the criterion for transition from axisymmetry to tripolar structures, the intensity of the cyclonic vortex was varied systematically. This could be conveniently done by varying the difference in level ( $\Delta H$ ) of the fluid on either side of the inner cylinder. The flow was visualized by dyeing the fluid in the inner cylinder and by using tracer particles floating on the free surface; observations were made both photographically and by eye. In the experiments  $\Delta H$  was varied between its maximum value (empty inner cylinder) to approximately  $0.2\bar{H}$ , with  $\bar{H}$  the mean water depth, measured at rest after the experiment. Except for  $\bar{H}$ , which was varied from 5.0 to 21.8 cm, all other experimental parameters were kept constant, i.e.  $\Omega = 1.0 \text{ s}^{-1}$  and the diameter of the inner cylinder  $2R_0 = 29.0 \text{ cm}$ . The observational data obtained from some 35 experiments on cyclonic vortices are presented graphically in figure 9. In this graph the open circles represent experiments in which a transition to tripoles was observed, whereas the black dots denote experiments in which the vortex remained circularly symmetric or became slightly elliptic (in the observations by eye, the difference between circular and slightly elliptic vortices is hardly discernible). Tripole-like vortices with extremely weak satellite vortices are denoted by squares in figure 9. In such weak tripoles two very thin, elongated regions of anticyclonic vorticity are observed to be compressed against the cyclonic core, which is in such cases almost circular. So there is in fact a continuous range of forms: a tripole like the one shown in figure 3 is found at one end of this range, while the stable, circularly symmetric vortex is found at the other end.

Usually, the observation period lasted as long as there were observable motions, and the type classification indicates what kind of streamline pattern is observed just before velocities fall below measurable levels. For relatively small values of  $\bar{H}$  and  $\Delta H/\bar{H}$  (lower left corner in figure 9) a transition to a clearly discernible, strong tripole is observed to occur within a period approximately equal to the Ekman time, while the stronger vortices for relatively large values of  $\bar{H}$  (upper right corner in figure 9) stayed close to circular even after a period equal of two or three times the Ekman time. The evolution of these stable vortices is discussed in Kloosterziel & van Heijst (1990), where it is shown that the 'collapse'-produced stable vortices asymptotically (in time) get very close to a state in which the azimuthal velocity distribution is well approximated by the following profile:

$$v_{\text{stir}}(r) = \frac{1}{2}U'(r/L') \exp(-\frac{1}{2}(r/L')^2), \quad (1)$$

for which the corresponding vorticity distribution is given by

$$\omega_{\text{stir}}(r) = (U'/L')(1 - \frac{1}{2}(r/L')^2) \exp(-\frac{1}{2}(r/L')^2). \quad (2)$$

Here  $U'$  and  $L'$  are respectively an appropriate velocity scale and lengthscale. But measurements of the velocity profile of stirred vortices prior to transforming into tripoles revealed, to a high degree of precision, the same velocity distribution. The fact that the stirring vortices just before transforming into tripoles are very close to this particular form too thus seems to indicate that this state in some sense draws a line between stable and unstable flow profiles.

In the next section a critical Rossby number is derived for this vortex structure, which, if exceeded, is expected to lead to centrifugal instabilities. If the Rossby number of a particular vortex is far below this critical value, it appears that tripole formation is a manifestation of the instability of the vortex to two-dimensional perturbations. Isolated vortices like the vortex with the velocity distribution above given, all satisfy Rayleigh's inflexion-point theorem, which is a necessary but not sufficient condition for instability with respect to two-dimensional perturbations (see Drazin & Reid 1981). It was observed in many experiments (see Kloosterziel & van Heijst 1990) that the collapse-produced monopolar vortices have a slowly changing velocity and vorticity distribution, this being induced by the Ekman circulation. Although the initial monopolar vortex might be stable in itself, its vorticity distribution can thus be modified slowly in such a way that the vortex eventually becomes unstable. Roughly stated, instability requires that the amplitude of the vorticity minimum relative to the core maximum has to exceed some critical value. For certain simple model vortices criteria of this kind are derived by Flierl (1988).

For relatively small values of  $\bar{H}$  and  $\Delta H/\bar{H}$  the motion is observed to be confined to a region small compared with the tank width and to have a rather narrow ring of strong negative vorticity around the core, whereas for larger values of  $\bar{H}$  and  $\Delta H/\bar{H}$  the stronger vortices are observed to be much wider and to have a much wider region of small-amplitude negative vorticity relative to the size of the positive-vorticity core. In the former case a fraction of the Ekman time is needed to bring the vortex close to the critical form, owing to the Ekman circulation, and enough energy is left then to have an observable transition to the tripolar form, due to the growth of wavenumber-2 instabilities; in the latter case so much time is needed to bring the vortex to this form that by then the vortex may have been entirely dissipated. The above-mentioned weak tripoles fall somewhere in between these two possibilities: not enough energy is left then in these cases for the satellite vortices to grow appreciably.

In an attempt to produce anticyclonic barotropic vortices, the same collapse technique was applied with the fluid level inside the inner cylinder higher than outside. It was found, however, that no vortex forms after lifting the inner cylinder: the resulting flow appeared to be highly irregular, and no well-defined structures could be recognized.

#### 4. Stability considerations

During the course of the experimental work it was noted that it is virtually impossible to create *anticyclonic* vortices in the rotating tank if one attempts to do so by simply stirring the fluid locally. But cyclonic vortices are easily created in this way! In the anticyclonic case stirring does not lead to any well-defined, organized vortex flow – it leads to turbulent motion and the generation of waves – whereas from cyclonic stirring a well-defined smooth vortex forms. If such vortices are initially generated in a bottomless cylinder and subsequently released, then the cyclones transform into tripoles while at all times showing Taylor-column motion. During the evolution towards this state, all motion appears highly synchronized in the vertical direction; this implies that the tripole formation is close to two-dimensional. It is observed, however, that the instabilities of anticyclones as described in §3.1 involve strong vertical motions and lead to vigorous turbulent mixing. The flow rapidly ‘self-organizes’, and during this process the dipoles form. When viewed from the side, these dipoles look like a combination of two counter-rotating columns, and their motion is by then two-dimensional too.

So, in general the instabilities of cyclones appear to be non-axisymmetric two-dimensional ones, whereas those of anticyclones are often three-dimensional. This difference is not fully understood yet, but some results partially explaining the difference are presented below. Later in this section critical Rossby numbers are derived for two different vortex structures: for the isolated vortex with a flow profile given by (1) and for a non-isolated vortex which, under typical laboratory circumstances, was never observed to become unstable if cyclonic. These Rossby numbers provide a threshold value beyond which Rayleigh’s circulation theorem is satisfied. This theorem states that a sufficient condition for instability is that the circulation decreases in magnitude somewhere in the vortex. If these critical values are exceeded, centrifugal instabilities will ensue in the form of *axisymmetric* overturning motion. For cyclones these critical numbers are much higher than for anticyclones, and this gives a satisfactory explanation for the difficulties one has with generating anticyclones by stirring in an unconfined region.

The critical Rossby number for anticyclones is rather small, and in most experiments with anticyclonic stirring vortices this number was – unintentionally – exceeded. Assuming that the stirred vortices of both kinds have the same flow profile prior to releasing them (this will only be so if one quickly withdraws the cylinder after the stirring has been stopped), the only difference would be their absolute angular momentum, and this is a determining factor only for three-dimensional centrifugal instabilities. The explosive character of the instabilities that set in when anticyclones are released and the relative calm way cyclones evolve (they usually do not exceed the critical Rossby number) indicate that part of the subsequent evolution of anticyclones involves centrifugal instabilities.

To differentiate between the different possible instability types is difficult. For instance, if the critical Rossby number is exceeded, axisymmetric perturbations *will* grow, while simultaneously three-dimensional non-axisymmetric perturbations and

two-dimensional non-axisymmetric perturbations *may* grow (for the latter type of instabilities, the relative flow has to satisfy Rayleigh's inflexion-point theorem). All these instabilities are competing and without further research one cannot tell which is the fastest-growing mode. It may well be that a vortex is unstable to two-dimensional perturbations with wavenumber 2, to three-dimensional perturbations with wavenumber 3 and at the same time (if the critical number is exceeded) show overturning motions. Which mode is observed depends on the relative growth rate of each unstable mode.

Tripole formation has recently been observed in numerical simulations of two-dimensional flows (see Carton *et al.* 1989) as well as dipole splitting (see Flierl 1985, 1988 and Stern 1987, among others), and in all cases this was the result of the growth of wavenumber-2 perturbations. In the laboratory, the tripole formation appears to be covered by the two-dimensional theory, but during dipole splitting a 'mix' of both two-dimensional instabilities and overturning (vertical) motions is observed (this may well be a single three-dimensional, non-axisymmetric mode too). For this difference no satisfactory theory has been developed. The normal-modes analysis of Chandrasekhar (1961) can be extended straightforwardly to the  $f$ -plane or the rotating-tank case, and, with respect to non-axisymmetric three-dimensional perturbations, the following can be said. If the critical Rossby numbers are exceeded, both cyclones and anticyclones will have growing non-axisymmetric modes too. For high enough Rossby numbers therefore, axisymmetric overturning motions *and* three-dimensional non-axisymmetric motions will ensue. One cannot tell which will be dominant from the normal-modes analysis without actually constructing these modes; this poses insurmountable problems and the analysis therefore stops at this point. For cyclones the critical Rossby number is usually not exceeded, and the results to be derived below show that axisymmetric instabilities (overturning motions) will not grow, but according to Chandrasekhar (1961) it remains an open question whether three-dimensional, non-axisymmetric perturbations will amplify or not. So even if a cyclone or anticyclone has a Rossby number below the critical value, three-dimensional non-axisymmetric perturbations may grow, but proving this is difficult. The two-dimensional character of the tripole formation favours the option that cyclones are stable to these perturbations, and that the flow evolution is essentially two-dimensional.

In some experiments anticyclonic isolated vortices were left for a while in the inner cylinder until the estimated Rossby number was near or below the critical value. When these vortices were released two different things could happen. In many cases again dipole splitting occurred, but in some other cases a triangular vortex formed (see §3.1). Since purely overturning instabilities are excluded in this case, these scenarios can be manifestations of either two- or three-dimensional non-axisymmetric instabilities. It is not known which mode is the most unstable one, and much remains to be answered here. The fact that two-dimensional numerical simulations show such a striking resemblance to the laboratory observations of dipole splitting (see Flierl 1985, 1988) indicate that at least part of the evolution is due to the growth of two-dimensional perturbations.

If one assumes that all vertical motion is zero at all times, one enters purely two-dimensional theory in which there is no difference between cyclones and anticyclones. Rayleigh's inflexion-point criterion applies in this case, and it follows that a necessary condition for instability is that the gradient of the vorticity changes sign somewhere; the amplitude or sign of the flow is of no importance. All isolated vortices satisfy this criterion. Both Rayleigh's circulation theorem (three-dimensional flows)

and Rayleigh's inflexion point criterion (two-dimensional flows) provide conditions that have to be satisfied if perturbations are to grow or not, but they do not reveal which type of perturbation is the fastest growing one.

For smooth velocity profiles like that given by (1), a normal-modes analysis proves to pose a very complicated analytical problem, and such a profile is therefore usually tested for its (linear) stability properties by means of some numerical analysis (an exception is the analytical treatment of Flierl (1988) concerning the stability of vortices with piecewise-constant vorticity). An example is Gent & McWilliams' (1986) analysis of several smooth flow profiles for which the fastest-growing modes were determined by means of a finite-differences method. According to their study the profile given by (1) is unstable to wavenumber-2 perturbations only, and this appears to be in accordance with the observed tripole formation linked to this profile type (a Galerkin method in Kloosterziel (1990) predicts a wavenumber-3 perturbation to be the fastest-growing mode for this vortex; a reason for this conflict in results has as yet not been found).

### *Centrifugal instability*

Rayleigh's circulation theorem states that in the absence of viscosity a necessary and sufficient condition for a stationary swirling flow, with an azimuthal velocity distribution  $v(r)$ , to be stable to axisymmetric disturbances is that the square of the circulation does not decrease anywhere, i.e.

$$\frac{d}{dr}(vr)^2 \geq 0 \quad (3)$$

(see Drazin & Reid 1981, or Chandrasekhar 1961), whereas the flow is unstable if it decreases somewhere. Rayleigh (1916) invoked an energy argument in which two concentric fluid rings were imagined to be interchanged while conserving their angular momentum. By comparing the kinetic energy before and after the exchange, it followed that if (3) is satisfied, the kinetic energy increases. In such cases then, without a source of energy such an event would never occur spontaneously. On the other hand, if (3) is violated in some region the exchange would liberate energy and instability ensues.

Instead of using the energy argument, it is instructive to approach the question of stability by means of a 'displaced-particle' argument (an entirely analytic treatment is presented in Kloosterziel 1990). A fluid element is given a 'virtual displacement' in the prevailing force field and it is then checked whether it will accelerate or not, be 'pushed back' or not, thereby taking the force field, which is here the pressure gradient, as unaltered and undisturbed by the motion of the fluid element.

In a rotating system that rotates with angular velocity  $\Omega$  – or on an  $f$ -plane – the equation for the azimuthal velocity of *circularly symmetric* flows reads

$$\frac{Dv}{Dt} + fu + \frac{uv}{r} = 0, \quad (4)$$

where  $u$  is, as usual, the radial velocity component,  $v$  the azimuthal component and  $f$  the Coriolis parameter. For a rotating tank  $f = 2\Omega$ . The material derivative is defined here as

$$\frac{D}{Dt} = \frac{\partial}{\partial t} + u \frac{\partial}{\partial r} + w \frac{\partial}{\partial z},$$

where  $w$  is the vertical velocity component. Equation (4) implies the following conservation law :

$$\frac{D}{Dt}(vr + \frac{1}{2}fr^2) = 0. \quad (5)$$

For a vortex located at the centre of the rotating tank the term within the brackets is the absolute angular momentum, or circulation, of a revolving fluid element at radius  $r$ . The equation for the radial velocity component is

$$\frac{Du}{Dt} - \frac{v^2}{r} - fv = -\frac{1}{\rho} \frac{\partial p}{\partial r}. \quad (6)$$

If the stationary basic vortex whose stability is under study has an azimuthal velocity distribution  $v_0(r)$ , the pressure-gradient force is necessarily

$$\frac{1}{\rho} \frac{dp_0}{dr} = \frac{v_0^2}{r} + fv_0. \quad (7)$$

If a fluid element is imagined to change its position slightly, from, say,  $r_0$  to  $r' = r_0 + \delta r$ , it will acquire an azimuthal velocity  $v'(r')$  that is determined by the conservation law expressed by (5):

$$v'(r')r' + \frac{1}{2}fr'^2 = v_0(r_0)r_0 + \frac{1}{2}fr_0^2. \quad (8)$$

This holds only for flows that are axisymmetric, and axisymmetry can only hold when all motion takes place in the form of an exchange of rings; this necessarily involves three-dimensional *overturning* motions.

Assuming that the prevailing pressure field is not changed by the motion, the element experiences an acceleration

$$\frac{D^2\delta r}{Dt^2} = \left\{ \frac{v'^2}{r'} + fv' \right\} - \left\{ \frac{v_0^2}{r} + fv_0 \right\}, \quad (9)$$

where  $v_0$  is understood to be evaluated at  $r = r'$ . Taking (8) into account, the right-hand side is found to be equal to

$$\frac{1}{r'^3} \{ (v_0(r_0)r_0 + \frac{1}{2}fr_0^2)^2 - (v_0(r')r' + \frac{1}{2}fr'^2)^2 \}.$$

If this is developed in a Taylor series around  $r = r_0$ , one obtains

$$\frac{D^2\delta r}{Dt^2} = -\frac{\delta r}{r_0^3} \frac{d}{dr} (v_0 r + \frac{1}{2}fr^2)^2|_{r_0} + O(\delta r^2). \quad (10)$$

Assume, for example, that  $\delta r$  is positive ( $\delta r = u\delta t$ ;  $u > 0$ ), then this equation tells us that there is a tendency to accelerate it even farther away from its original position if, for some  $r_0$ ,

$$\frac{d}{dr} (v_0 r + \frac{1}{2}fr^2)^2 < 0. \quad (11)$$

Note that Rayleigh's original criterion is regained if one lets  $f \rightarrow 0$ . The criterion expressed by (11) could have been directly inferred from (3) if one has in mind vortices that are located exactly at the centre of the rotating tank, since in that case one can read for  $v$  in (3) the absolute velocity  $v + \Omega r$ . The criterion derived here is

valid for vortices on an  $f$ -plane as well as for vortices that are off-centre in a rotating fluid system (for such vortices (4) and (6) are valid too). Spatially varying depth effects and free-surface effects have been assumed to be of negligible importance under typical laboratory conditions.

Introducing a velocity scale  $U$ , equal to, say, the maximum velocity, and a lengthscale  $L$ , which can for instance be the position of maximum velocity, the criterion is, in non-dimensional terms,

$$(\epsilon\tilde{v} + R)(\epsilon\tilde{\omega} + 2) > 0 \rightarrow \text{stable}, \quad (12)$$

$$(\epsilon\tilde{v} + R)(\epsilon\tilde{\omega} + 2) < 0 \rightarrow \text{unstable}, \quad (13)$$

where  $\tilde{v}$  is the dimensionless velocity  $\tilde{v} = v/U$ ,  $\tilde{\omega}$  the dimensionless relative vorticity  $\tilde{\omega} = \omega/(U/L)$  and the Rossby number  $\epsilon = U/(\Omega L)$ . Rayleigh's modified criterion thus states that a vortex is stable if the product of absolute vorticity and 'absolute' velocity (on an  $f$ -plane  $\epsilon\tilde{v} + R$  cannot be interpreted as the absolute velocity) is positive everywhere, or, alternatively, that they be of the same sign everywhere. Instability is found if the vorticity and velocity differ in sign somewhere. In particular, this implies that in an inertial frame ( $\Omega = 0$  or  $f = 0$ ), where (3) applies, in an unbounded domain stable vortices are those with single-signed vorticity (having non-vanishing circulation for  $r \rightarrow \infty$ ), whereas all vortices with vanishing circulation ('isolated vortices') and single-signed velocity are unstable. The exact sign is of no importance, of course. A typical stirring vortex is an isolated vortex and, as a simple experiment shows, such a vortex will not persist if it is created in a (non-rotating) container that has a diameter much larger than the region that is stirred (in a tea cup the walls play a stabilizing role, but in a large container stirring merely leads to turbulent and wavy motion).

In a rotating system or on an  $f$ -plane the sense of rotation of the vortex is important as the criterion stated by (12), (13) shows. There is no symmetry in the sense that a vortex with some specific velocity profile can be stable if it is a cyclone, whereas it is unstable if anticyclonic. This is elucidated by the following examples. Two reference cases will be considered; that of a stirred vortex with the velocity and vorticity given by (1) and (2), respectively, and that of a vortex with a velocity profile

$$v_{\text{sink}}(r) = U' \frac{1}{(r/L')} \{1 - \exp(-\frac{1}{2}(r/L')^2)\} \quad (14)$$

and corresponding vorticity

$$\omega_{\text{sink}}(r) = (U'/L') \exp(-\frac{1}{2}(r/L')^2). \quad (15)$$

The subscript 'sink' refers to the fact that these profiles are representative of a class of laboratory vortices created with the so-called sink technique (see Kloosterziel & van Heijst 1990). The sink vortex is an example of a non-isolated vortex with infinite energy on an unbounded domain while the stirred vortex is a truly isolated vortex with vanishing circulation for larger radii and finite energy. In order to illustrate the consequences of the non-dimensional criterion stated above, the velocity profiles are scaled such as to have  $\tilde{v}_{\text{max}} = 1$  and  $R_{\text{max}} = 1$ . The Rossby number is thus based on position and amplitude of the peak velocity. In figures 10 and 11 the product  $(\epsilon\tilde{v} + R)(\epsilon\tilde{\omega} + 2)$  is shown as a function of  $R$  for these two cases while differentiating between the cyclonic and the anticyclonic cases: the Rossby number has been given the values 0.5, 2 and 5. Instability is recognized where the product takes negative values. It is seen in figure 10 that the non-isolated vortex, which in an inertial frame

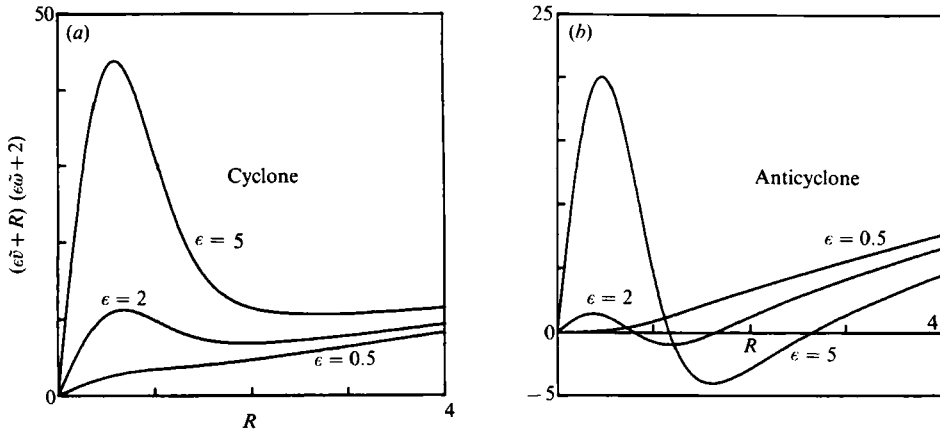


FIGURE 10. The product of the non-dimensional absolute vorticity and velocity as a function of the dimensionless radius  $R$  of the vortex, with velocity and vorticity given by (14) and (15), for (a) the cyclonic and (b) the anticyclonic case. This is a characteristic example of a *non-isolated* vortex for which the circulation does not vanish at large radii. The Rossby number has been given the values  $\epsilon = 0.5, 2$  and  $5$ . In the region where the product is negative, centrifugal instabilities are expected. Only anticyclones of this type will be unstable if a critical Rossby number is exceeded (see text).

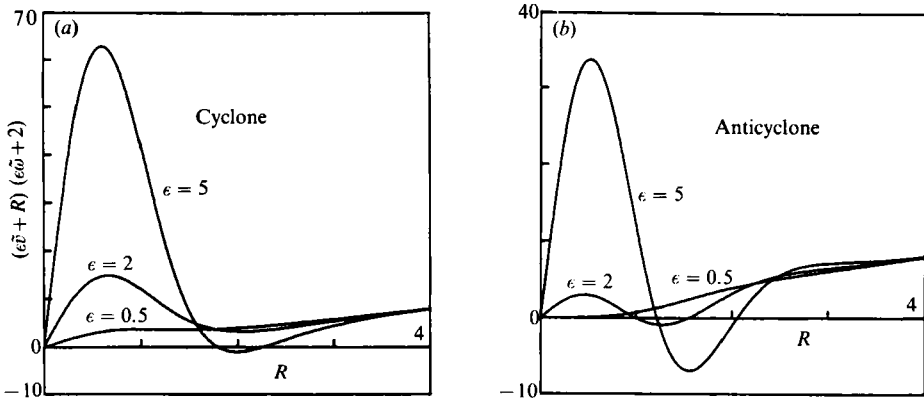


FIGURE 11. The product of the non-dimensional absolute vorticity and velocity as a function of the dimensionless radius  $R$  of the stirred vortex, with velocity and vorticity given by (1) and (2), for (a) cyclones and (b) anticyclones. This is an example of an *isolated* vortex, i.e. a vortex with vanishing circulation. The Rossby number has been given the values  $\epsilon = 0.5, 2$  and  $5$ . Both cyclonic and anticyclonic vortices are unstable if a critical Rossby number is exceeded (see text).

would be stable irrespective of amplitude or scale, in the cyclonic case is stable for any Rossby number too, but in the anticyclonic case it becomes unstable if the Rossby number exceeds a critical value that is approximately  $\epsilon_{\text{crit}} \approx 0.57$ . The isolated vortex can be unstable in both the cyclonic and anticyclonic case, as figure 11 indicates. For the cyclone the critical Rossby number is  $\epsilon_{\text{crit}} \approx 4.5$  whereas for the anticyclone it is  $\epsilon_{\text{crit}} \approx 0.65$ . Although the value of the critical Rossby number does depend to a large extent on the exact structure of the vortex considered, a simple rule of thumb can be inferred from these results: only very *weak anticyclones* are centrifugally *stable* in a rotating system whereas only very *strong cyclones* are centrifugally *unstable*.

All this is in accordance with the observation that it is rather hard to generate

persistent anticyclones since one usually exceeds quite easily (and unintentionally) a critical forcing level. Consider for instance the cyclonic stirring vortex. If one assumes that the maximum velocity occurs at a radius  $r_{\max} = 4$  cm, such a cyclone would still be stable if the amplitude was  $18 \text{ cm s}^{-1}$ ! On the other hand, an anticyclone – with a maximum at the same position – is unstable if the amplitude exceeds a value of about  $2.5 \text{ cm s}^{-1}$  (approximately one revolution of a fluid element in 10 s, which is very slow). Another interesting difference between these two cases is that manifestations of centrifugal instabilities (in the form of overturning motions) in the cyclone will take place in a region around  $r = 2r_{\max}$ , which is at the edge of the vortex, whereas in anticyclones that have a Rossby number that just barely exceeds the critical point the region is right in the core; for increasing Rossby number it shifts outward.

The cyclonic sink vortices were never observed to become unstable, irrespective of the different levels of forcing used (see Kloosterziel & van Heijst 1990). On the other hand, it was noted that one could create anticyclones by reversing the procedure, that is, by injecting fluid into the rotating fluid layer, but only if very low volume fluxes are maintained, i.e. if the Rossby number is kept very small (Griffiths & Hopfinger 1987 estimated the Rossby number of their (stable) anticyclonic sink vortices initially to be approximately 0.15).

In a recent study it was shown by Bayly (1988) that Rayleigh's circulation theorem (in an inertial frame) can be extended to a large class of monopolar vortices. For vortices consisting of a set of nested convex closed streamlines, a sufficient condition for instability to three-dimensional centrifugal instabilities is that the circulation along a streamline decreases outward in strength somewhere. This can probably be extended without much difficulty to rotating systems, and, say, elliptical cyclones of moderate strength would then be stable whereas their anticyclonic counterparts would again be unstable. Circular symmetry therefore need not be enforced, as was done in this section.

## 5. Conclusions

The laboratory experiments described in this paper demonstrate the remarkable difference between unstable cyclonic and anticyclonic vortices in a rotating homogeneous fluid, both in their instability *behaviour* and in the actual *conditions* for instability.

An unstable cyclonic vortex was observed to show a gradual transition into a stable tripolar structure consisting of a core of positive vorticity, adjoined by two weaker satellite vortices with negative vorticity. In contrast, an anticyclonic barotropic vortex generally shows an 'explosive' instability behaviour, in the sense that it immediately splits up into two dipolar vortices which rapidly move away from the original vortex centre. In addition to this dipole splitting of an unstable anticyclone, another behaviour was observed in a few cases, viz. the higher-order mode 3-instability which consists of a triangular anticyclonic core vortex with three smaller cyclonic satellite vortices beside it. In the experiments this mode was not stable, however, and the structure showed a rapid transition into an anticyclonic tripole, which in turn became unstable and split up into two dipolar vortices.

Whether an initially axisymmetric vortex is unstable or not depends on its vorticity distribution as well as on the value of the Rossby number characterizing the vortex strength. An extension of Rayleigh's original instability analysis to a rotating system or an  $f$ -plane (§4) provides a criterion, which is that a vortex is centrifugally

stable if the product of absolute vorticity and absolute velocity is positive everywhere. The background rotation in the system obviously causes symmetry breaking, and the rotation sense of the vortex is therefore an important factor in the instability criterion. In order to examine the role of the vorticity distribution in the vortex instability, examples of two different vortex types were considered, viz. an isolated and a non-isolated vortex (corresponding with laboratory vortices generated by the 'stirring' and the 'sink' technique, respectively). In the latter case it was found that a cyclonic vortex is stable for all Rossby numbers, whereas its anticyclonic counterpart becomes centrifugally unstable when the Rossby number exceeds some (small) critical value. On the other hand, an isolated vortex was found to be unstable both in the cyclonic and the anticyclonic case, but for completely different values of the Rossby number. Although the value of the critical Rossby number depends to a large extent on the structure of the vortex considered, the results of the analysis can be expressed as the following approximate rule of thumb: only very weak anticyclonic vortices are centrifugally stable, whereas only very strong cyclonic vortices are centrifugally unstable. The laboratory observations agree very well with this rule, at least in a qualitative sense.

A number of the experiments described in this paper were carried out on a direct-drive turntable that was built more or less as a duplicate of a rotating table in use at the Department of Applied Mathematics and Theoretical Physics, University of Cambridge, UK. We are very grateful to Dr Paul F. Linden for his courtesy and his kind willingness to provide us with the required technical instructions and specifications. One of us (R. C. K.) gratefully acknowledges financial support from the working group on Meteorology and Physical Oceanography (MFO) of the Netherlands Organization of Scientific Research (NWO).

## REFERENCES

- BAYLY, B. J. 1988 Three-dimensional centrifugal-type instabilities in inviscid two-dimensional flows. *Phys. Fluids* **31**, 56–64.
- CARNEVALE, G. F., KLOOSTERZIEL, R. C. & HEIJST, G. J. F. VAN 1990 Propagation of barotropic vortices over topography in a rotating tank. *J. Fluid Mech.* (submitted).
- CARNEVALE, G. F., VALLIS, G. K., PURINI, R. & BRISCOLINI, M. 1988 Propagation of barotropic modons over topography. *Geophys. Astrophys. Fluid Dyn.* **41**, 45–101.
- CARTON, X. J., FLIERL, G. R. & POLVANI, L. M. 1989 The generation of tripoles from unstable axisymmetric isolated vortex structures. *Europhys. Lett.* **9**, 339–344.
- CARTON, X. J. & McWILLIAMS, J. C. 1989 Barotropic and baroclinic instabilities of axisymmetric vortices in a quasi-geostrophic model. In *Mesoscale/Synoptic Coherent Structures in Geophysical Turbulence* (ed. J. C. J. Nihoul & B. M. Jamart), pp. 225–244. Elsevier.
- CHANDRASEKHAR, S. 1961 *Hydrodynamic and Hydromagnetic Stability*. Oxford University Press.
- CUSHMAN-ROISIN, B., HEIL, W. H. & NOF, D. 1985 Oscillations and rotations of elliptical warm-core vortices. *J. Geophys. Res.* **90**, 11756–11764.
- DRAZIN, P. G. & REID, W. H. 1981 *Hydrodynamic Stability*. Cambridge University Press.
- FLIERL, G. R. 1985 Instability of vortices. *Woods Hole Oceanogr. Inst., Tech. Rep.* WHOI-85-36, pp. 119–121.
- FLIERL, G. R. 1988 On the instability of geostrophic vortices. *J. Fluid Mech.* **197**, 349–388.
- GENT, P. R. & McWILLIAMS, J. C. 1986 The instability of circular vortices. *Geophys. Astrophys. Fluid Dyn.* **35**, 209–233.
- GINSBURG, A. I., KOSTIANOV, A. G., PAVLOV, A. M. & FEDOROV, K. N. 1987 Laboratory reproduction of mushroom-like currents (vortex dipoles) under rotation and stratification conditions. *Izv. Akad. Nauk. SSSR Atmos. Ocean. Phys.* **23**, 170–178.

- GRIFFITHS, R. W. & HOFFINGER, E. J. 1987 Coalescing of geostrophic vortices. *J. Fluid Mech.* **178**, 73–97.
- GRIFFITHS, R. W. & LINDEN, P. F. 1981 The stability of vortices in a rotating, stratified fluid. *J. Fluid Mech.* **105**, 283–316.
- HEIJST, G. J. F. VAN & KLOOSTERZIEL, R. C. 1989 Tripolar vortices in a rotating fluid. *Nature* **338**, 569–571.
- HEIJST, G. J. F. VAN, KLOOSTERZIEL, R. C. & WILLIAMS, C. W. M. 1991 Laboratory experiments on the tripolar vortex in a rotating fluid. *J. Fluid Mech.* (to appear).
- HOLTON, J. R. 1979 *An Introduction to Dynamic Meteorology* (2nd edn). Academic.
- IKEDA, M. 1981 Instability and splitting of mesoscale rings using a two-layer quasi-geostrophic model on an  $f$ -plane. *J. Phys. Oceanogr.* **11**, 987–998.
- KLOOSTERZIEL, R. C. 1990 Barotropic vortices in a rotating fluid. Ph.D. thesis, University of Utrecht, The Netherlands.
- KLOOSTERZIEL, R. C. & HEIJST, G. J. F. VAN 1989 On tripolar vortices. In *Mesoscale/Synoptic Coherent Structures in Geophysical Turbulence* (ed. J. C. J. Nihoul & B. M. Jamart), pp. 609–625. Elsevier.
- KLOOSTERZIEL, R. C. & HEIJST, G. J. F. VAN 1990 The evolution of stable barotropic vortices in a rotating free-surface fluid. *J. Fluid Mech.* (submitted).
- LEGRAS, B., SANTANGELO, P. & BENZI, R. 1988 High-resolution numerical experiments for forced two-dimensional turbulence. *Europhys. Lett.* **5**, 37–42.
- LEITH, C. E. 1984 Minimum enstrophy vortices. *Phys. Fluids* **27**, 1388–1395.
- MCWILLIAMS, J. C. & GENT, P. R. 1986 The evolution of sub-mesoscale, coherent vortices on the  $\beta$ -plane. *Geophys. Astrophys. Fluid Dyn.* **35**, 235–255.
- MORY, M., STERN, M. E. & GRIFFITHS, R. W. 1987 Coherent baroclinic eddies on a sloping bottom. *J. Fluid Mech.* **183**, 45–62.
- POLVANI, L. M. & CARTON, X. J. 1990 The tripole: a new coherent vortex structure of incompressible two-dimensional flows. *Geophys. Astrophys. Fluid Dyn.* **52**, 87–102.
- RAYLEIGH, LORD 1916 On the dynamics of revolving fluids. *Proc. R. Soc. Lond. A* **93**, 148–154.
- ROBINSON, A. R. (Ed.) 1983 *Eddies in Marine Science*. Springer.
- SAUNDERS, P. M. 1973 The instability of a baroclinic vortex. *J. Phys. Oceanogr.* **3**, 61–65.
- STERN, M. E. 1987 Horizontal entrainment and detrainment in large-scale eddies. *J. Phys. Oceanogr.* **17**, 1688–1695.
- SWENSON, M. 1987 Instability of equivalent barotropic riders. *J. Phys. Oceanogr.* **17**, 492–506.